

Fig. 3 Total emissivity of temperature-fluctuating carbon dioxide-water vapor mixture. The partial pressures of carbon dioxide and water vapor are, respectively, 0.1013 bar, the total pressure is 1.013 bar.

sivity may be more appreciably raised with α than that obtained in the present analysis.

Conclusions

- 1) For \bar{T} greater than about 1500 K, the effect of α on the total emissivity diminishes with an increase in \bar{T} , irrespective of a value of the pressure-path length product and kinds of infrared gas.
- 2) The total emissivity of a carbon dioxide layer with \bar{T} less than about 1500 K increases with α over the whole range of pressure-path length product. This is the case for a carbon dioxide and water vapor mixture.
- 3) The total emissivity of a water vapor layer with \bar{T} less than about 1500 K appreciably increases with α , except at a small pressure-path length product.

Acknowledgment

The author expresses his sincere gratitude to T. F. Smith for his valuable comments on the original manuscript.

References

- ¹Cox, G., "On Radiant Heat Transfer from Turbulent Flames," *Combustion Science and Technology*, Vol. 17, 1977, pp. 75-78.
- ²Gore, J. P., Jeng, S.-M., and Faeth, G. M., "Spectral and Total Radiation Properties of Turbulent Hydrogen/Air Diffusion Flames," *Journal of Heat Transfer*, Vol. 109, No. 1, 1987, pp. 165-171.
- ³Gore, J. P., Jeng, S.-M., and Faeth, G. M., "Spectral and Total Radiation Properties of Turbulent Carbon Monoxide/Air Diffusion Flames," *AIAA Journal*, Vol. 25, No. 2, 1987, pp. 339-345.
- ⁴Song, T. H., and Viskanta, R., "Interaction of Radiation with Turbulence: Application to a Combustion System," *Journal of Thermophysics and Heat Transfer*, Vol. 1, No. 1, 1987, pp. 56-62.
- ⁵Soufiani, A., Mignon, P., and Taine, J., "Radiation-Turbulence Interaction in Channel Flows of Infrared Active Gases," *Heat Transfer*, Vol. 6, Hemisphere, Washington, DC, 1990, pp. 403-408.
- ⁶Rotta, J., *Turbulent Strömungen*, B. G. Teubner, Stuttgart, Germany, 1972.
- ⁷Kamiuto, K., "Two-Parameter Wideband Spectral Model for the Absorption Coefficients of Molecular Gases," *Journal of Thermophysics and Heat Transfer*, Vol. 9, No. 3, 1995, pp. 569-573.
- ⁸Edwards, D. K., *Advances in Heat Transfer*, Vol. 12, Academic, New York, 1976, pp. 115-193.

Effect of Ribs with Holes on Heat Transfer in a Square Channel

S. C. Lau* and R. B. Spence†

Texas A&M University, College Station, Texas 77843

and

R. T. Kukreja‡

Lynntech, Inc., College Station, Texas 77840

Introduction

Gas turbine blades are subjected to intense heating by hot combustion gases. One way to maintain the blade wall temperatures below their melting points is to circulate cooling air through internal, rib-roughened passages.¹⁻³ Hwang and Liou^{4,5} showed that perforated and slit ribs improved the thermal performance of rib-roughened channels moderately better than solid ribs. However, when the small holes and slits on these ribs are clogged by dust particles or dirt in the flowing fluid the thermal performance of these ribs may be reduced significantly. The objective of this experimental investigation is to examine the effect of ribs with relatively large holes on the overall heat transfer and friction in heat exchanger flow passages. The finite number of jet streams passing through these holes on the ribs should disrupt flow reattachment and redevelopment on the channel wall, and should cause overall heat transfer and friction that are quite different from those in corresponding solid rib cases.

Test Apparatus

The test apparatus is an open airflow loop with a 7.6×7.6 cm square test channel that has two heated rib-roughened aluminum walls and two unheated smooth wooden walls. Each of the two heated walls has six identical segments arranged along the test channel and is heated with a flexible electric heater that is attached with adhesive to the outer surface of the wall. Thin rubber gaskets separate and thermally isolate adjacent wall segments. The test channel is heavily insulated to prevent extraneous heat losses to the surroundings.

The seven rib configurations considered are 4.8-mm square transverse aluminum ribs with no holes, five 1.6-mm-diam holes, and 11 1.6-mm-diam holes; 9.5-mm square ribs with no holes, five 4.8-mm-diam holes, and 11 1.6-mm-diam holes; and 9.5-mm square ribs with five 4.8-mm-diam holes sandwiched between six 1.6-mm-diam holes. Table 1 lists the configurations of the rib arrays.

The heater voltage drop and current are measured to determine the total power input. The average temperature of each segment is measured with imbedded thermocouples. The static pressure along the test channel is measured at six pressure taps that are installed along one of the unheated wooden walls. The pressures at a calibrated orifice flowmeter are measured to determine the air mass flow rate.

Overall average Nusselt number and friction factor results are determined for five Reynolds numbers between 9×10^3 and 4.3×10^4 , for each of the rib configurations listed in Table 1.

Data Reduction

The Reynolds number and the Moody friction factor, Re and f , respectively, are both defined based on the hydraulic diam-

Received Sept. 12, 1996; revision received Feb. 4, 1997; accepted for publication Feb. 4, 1997. Copyright © 1997 by the American Institute of Aeronautics and Astronautics, Inc. All rights reserved.

*Associate Professor, Mechanical Engineering.

†Research Assistant, Mechanical Engineering.

‡Research Engineer, 7610 Eastmark Drive.

Table 1 Geometries of ribs in this study

Case	Rib configuration	e/D_h , p/e	Number of holes, d/e	A_r
1	Solid ribs	0.0625, 10	—	—
1a	Ribs with holes	0.0625, 10	5, 0.33	0.027
1b	Ribs with holes	0.0625, 10	11, 0.33	0.060
2	Solid ribs	0.125, 10	—	—
2a	Ribs with holes	0.125, 10	5, 0.50	0.123
2b	Ribs with holes	0.125, 10	11, 0.17	0.030
2c	Ribs with holes	0.125, 10	5 + 6, 0.50 and 0.17	0.139

Note: e , height of ribs; p , pitch; d , diameter of holes on ribs; and A_r , hole area-to-rib frontal area ratio.

eter of the test channel, as in Incropera and DeWitt.⁶ The segmental heat transfer coefficient is calculated from the net heat transfer rate per unit projected surface area of a segment, the average wall temperature of the segment, and the local average bulk temperature (from the measured inlet air temperature, the mass flow rate, and the upstream net rate of heat transfer to the air). The net heat transfer rate is the electrical power generated by the heater, minus the conduction heat loss through the insulation, the net axial conduction heat loss, and the radiation loss.

The segmental Nusselt number is also based on the hydraulic diameter of the channel. The overall average Nusselt number \overline{Nu} is the average of the segmental Nusselt numbers of the second through the sixth segments of both heated walls. The slightly higher values of the segmental Nusselt numbers of the first segments that are caused by the entrance effect are neglected. The overall average Nusselt number is normalized with the Nusselt number for fully developed turbulent flow in a smooth tube Nu_0 , from Eq. (8.63a) in Incropera and DeWitt.⁶

To compare the overall heat transfer per unit pumping power for the ribbed channel with that for a tube, the relative thermal performance is calculated as

$$TP = (\overline{Nu}/Nu_0)(f/f_0)^{-1/3}$$

where f_0 is the friction factor for fully developed turbulent flow in a smooth tube [Eq. (8.63b) in Incropera and DeWitt⁶]. All properties of air are evaluated at the average of the bulk temperatures at the inlet and exit of the test section.

The maximum uncertainties (taking into consideration both bias and random errors, and using the method outlined in Coleman and Steele⁷) of the Reynolds number, the friction factor, the Nusselt number, and the thermal performance are estimated to be ± 7.3 , ± 16.0 , ± 9.6 , and $\pm 13.3\%$, respectively.

Presentation of Results

Overall heat transfer and friction results are presented in Fig. 1. With increasing Reynolds number, the friction factor ratios for the seven rib configurations increase, while the Nusselt number ratios and the relative thermal performances decrease. The larger ribs with $e/D_h = 0.125$ (open symbols) generally cause higher heat transfer and larger pressure drop than the smaller ribs with $e/D_h = 0.0625$ (darkened symbols). The larger ribs increase the heat transfer by a factor of 3.0–4.2 over that for turbulent flow in a smooth tube and the pressure drop by a factor of 5.7–10.7, whereas the smaller ribs cause the heat transfer and pressure drop to increase by 2.6–3.3 times and 2.7–5.6 times, respectively.

Holes on the ribs lower both the heat transfer and the pressure drop. In the case of the smaller ribs, increasing the number of holes from 5 to 11 in the ribs lowers both the heat transfer and the pressure drop. For the larger ribs, the five larger holes with $A_r = 0.123$ (case 2a) cause lower heat transfer and pressure drop than the 11 smaller holes with $A_r = 0.030$ (case 2b). The 11 holes of two sizes with $A_r = 0.139$ in case 2c give the lowest heat transfer and pressure drop among the four larger rib cases. Ribs with holes cause less overall friction to the flow, but the flow through the holes in the ribs interrupts

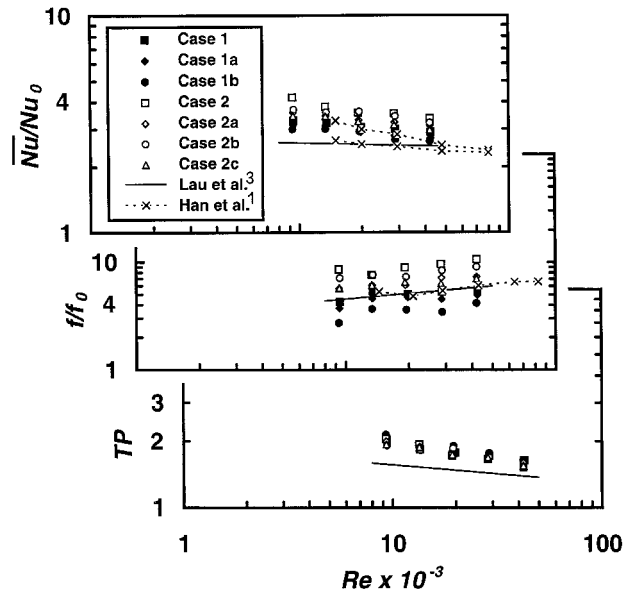


Fig. 1 Nusselt number ratio, friction factor ratio, and relative thermal performance results.

and weakens flow reattachment on the wall between the ribs, lowering the overall heat transfer.

Figure 1 shows that the friction factor results for the smaller solid ribs with $e/D_h = 0.0625$ (case 1) compare very well with corresponding predicted values based on a correlation by Lau et al.³ and results from Han et al.¹ The \overline{Nu}/Nu_0 distribution in case 1 is slightly higher (by up to 14%) than the corresponding distribution in the case of two unheated smooth walls from Han et al.¹ (upper dotted line with \times symbols). The \overline{Nu}/Nu_0 distributions for uniform heat flux on all four walls from Lau et al.³ (solid line) and Han et al.¹ (lower dotted line with \times symbols), which are also included in Fig. 1, are lower than all other distributions. These published values have been corrected using the correlation for Nu_0 given in the Data Reduction section.

For the seven rib configurations studied here, the relative thermal performance has values ranging from about 2.0 at $Re \approx 9.3 \times 10^3$ to about 1.6 at $Re \approx 4.2 \times 10^4$. Therefore, although the heat transfer enhancement is apparently offset by the pressure drop increase, the ribs manage to improve the thermal performance by 60–100% over the range of Reynolds number studied. While the holes on the ribs decrease the heat transfer and the pressure drop, they do not affect the thermal performance significantly. At any Reynolds number over the range studied, the values of TP for the seven rib configurations do not differ by more than 11.5%. Overall, the thermal performance of the smaller ribs with 11 holes (case 1b) is up to 6.7% higher than those of the other six rib configurations.

Published results by Hwang and Liou^{4,5} showed that ribs with many distributed small holes and long slits (with A_r values up to 0.44 and 0.46, respectively) enhanced more heat transfer and performed better than solid ribs, but not when A_r was smaller than 0.22. The results of this study are consistent with